Supplementary Data

Supplementary figure legends

Figure S1. *Localization of ATP13A2 in cerebral cortex of normal and PD brains.* Representative DAB immunostaining with ATP13A2 antibody (LMNR1) in the cingulate cortex of normal control or PD subjects. Staining indicates ATP13A2 localized to characteristic pyramidal neurons throughout cortical layers I to VI. Inset showing high magnification image of ATP13A2 immunostaining in cortical layer III pyramidal neurons indicating increased levels of ATP13A2 immunoreactivity in PD brains compared to control brains. Scale bar: 100 μm (inset: 20 μm).

Figure S2. *Increased levels of ATP13A2 in substantia nigra dopaminergic neurons of PD brains.* (A) Representative DAB immunostaning with ATP13A2 antibody (A9732, Sigma) in the substantia nigra pars compacta (SNpc) and cingulate cortex from normal control or PD subjects. Staining indicates ATP13A2 specifically localized to characteristic neuromelanin-positive dopaminergic neurons compared to a control section (no primary antibody), or to layer III cortical pyramidal neurons. (**B**) Representative DAB staining with ATP13A2 antibody (A3361, Sigma) in the SNpc from normal control and PD brains. Magnification is indicated.

Figure S3. *Silencing of ATP13A2 expression does not influence neurite outgrowth or apoptotic cell death of cortical neurons.* (**A**) Soluble extracts from HEK-293T cells transiently co-expressing untagged mouse ATP13A2 and rodent-specific ATP13A2 (sh-ATP13A2 #1 or #2) or non-silencing control (sh-control) shRNA-GFP GIPZ plasmids were probed with an antibody to ATP13A2 (LMNR1) to demonstrate shRNA-mediated silencing of ATP13A2. β-tubulin indicates equivalent protein loading. (**B** and **C**) Rat primary cortical neurons transfected at DIV 3 with shRNA-GFP (sh-control or sh-ATP13A2) plasmids alone, or with control empty vector and GFP plasmids at a 10:1 molar ratio to label transfected neurons. Cultures were fixed at DIV 7. (**B**) Representative fluorescent micrographs reveal the co-labeling of cortical neurons with GFP and microtubule-associated protein 2 (MAP2) for each condition. Merged images representing shRNA-GFP-expressing neurons were pseudo-colored with ICA to improve the contrast of neuritic processes for length measurements. Axonal processes are indicated by arrows. Scale bar:

400 μm. (C) Quantitative analysis of the length of GFP+/MAP2+ cortical neurites reveals no effect of ATP13A2 silencing on the length of axonal processes compared to control neurons (sh-control or empty vector). Bars represent the mean ± SEM length of GFP+ neurites in μm (n = 111-128 neurons/condition) sampled across three independent cultures. (**D**) Effect of ATP13A2 silencing on apoptotic cell death of cortical neurons. Primary cortical neurons were transfected with shRNA-GFP (sh-control or sh-ATP13A2) constructs at DIV 3 and fixed at DIV 7. Cultures were subjected to TUNEL staining and immunocytochemistry with anti-MAP2 antibody. TUNEL-positive neurons were counted as a percent of total GFP/MAP2-positive neurons and expressed as mean ± SEM (n = 3 experiments/cultures).

Figure S4. *Effect of WT and F182L ATP13A2 overexpression on mitochondrial fragmentation in neurons.* (**A**) Rat primary cortical neurons were co-transfected with V5-tagged human ATP13A2 (WT or F182L) or control empty vector and mito-DsRed2 plasmids at a 10:1 molar ratio at DIV 9 to label transfected neurons. At DIV 12, mito-DsRed2-labeled mitochondria in individual neurons were monitored by time-lapse, live-cell confocal microscopy. (**A**) Time-course of average mitochondrial length induced by acute cadmium exposure (at time 0 sec) indicating delayed cadmium-induced fragmentation in neurons overexpressing WT ATP13A2 but not F182L ATP13A2. Data were fitted to a second-order kinetic model. (**B**) F182L ATP13A2 overexpression modestly increases mean basal but not cadmium-induced (peak) mitochondrial length compared to control and WT ATP13A2 (*left graph*). WT ATP13A2 expression increases whereas F182L expression reduces the half-life ($t_{1/2}$) of cadmium-induced mitochondrial fragmentation compared to empty vector control (*right graph*). Data represents n = 9 neurons/condition sampled from 3 independent cultures. *P<0.05 compared to control condition assessed by unpaired Student's t-test. (**C**) Confocal fluorescence microscopy revealing equivalent cytoplasmic vesicular localization of V5-tagged human WT and F182L ATP13A2 transiently expressed in HEK-293T cells. Staining for ATP13A2 (red) and nuclei (DAPI, blue) are indicated. Confocal images are taken from a single z-plane at 0.15 μm thickness. Images are representative of at least two independent transfection experiments. Scale bar: 10 μm.

Figure S5. *Silencing of ATP13A2 expression promotes mitochondrial fragmentation in midbrain dopaminergic neurons.* (**A**) Rat primary midbrain cultures were co-transfected at DIV 3 with

shRNA (sh-control or sh-ATP13A2) and mito-GFP constructs at a 10:1 molar ratio to label transfected neurons. Cultures were fixed at DIV 7 and subjected to immunocytochemistry with anti-TH antibody to identify dopaminergic neurons. Confocal fluorescence microscopy reveals mitochondrial morphology in dopaminergic neurons, highlighting tubular (normal), intermediate (partially fragmented) or fragmented mitochondrial morphologies. (**B**) Quantitative analysis of mitochondrial fragmentation induced by ATP13A2 silencing in dopaminergic neurons. Mitochondria were subclassified as tubular, intermediate or fragmented in mito-GFP/TH-positive neurons expressing ATP13A2 shRNA (n = 27) or control shRNA (n = 24). Mitochondrial subclasses were expressed as a percent of the total number of mitochondria per condition sampled from two independent cultures.

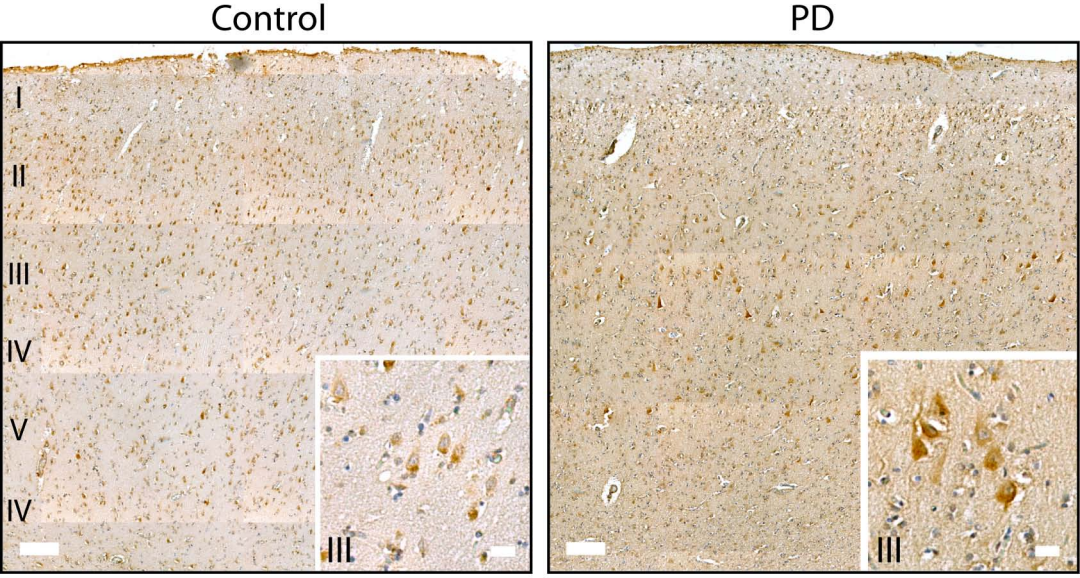

Cingulate cortex

Figure S1

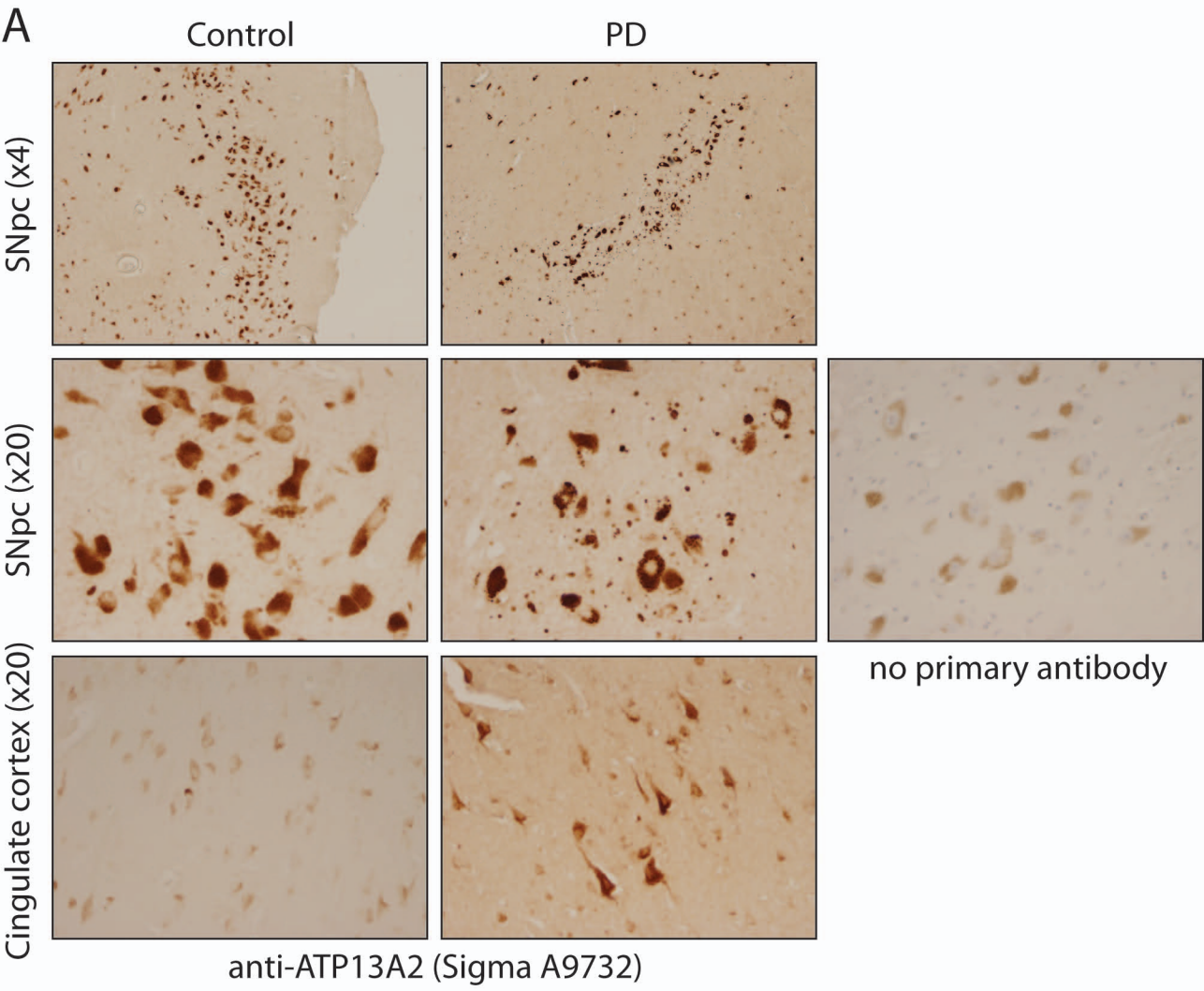
A
Control
PD
SNpc (x4)
SNpc (x20)
Cingulate cortex (x20)
no primary antibody
anti-ATP13A2 (Sigma A9732)

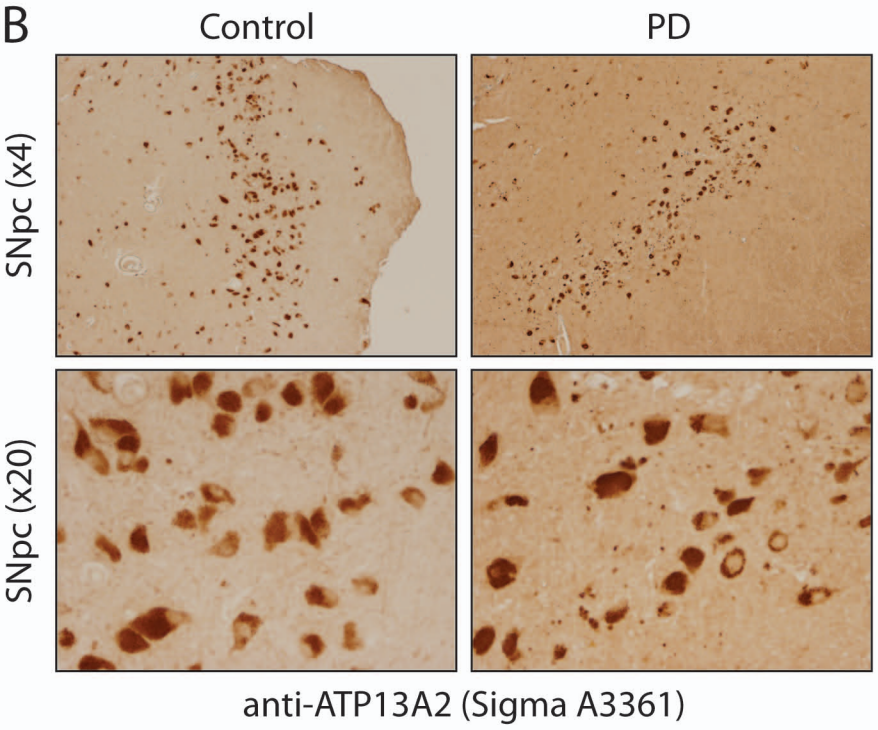
B
Control
PD
SNpc (x4)
SNpc (x20)
anti-ATP13A2 (Sigma A3361)

Figure S2

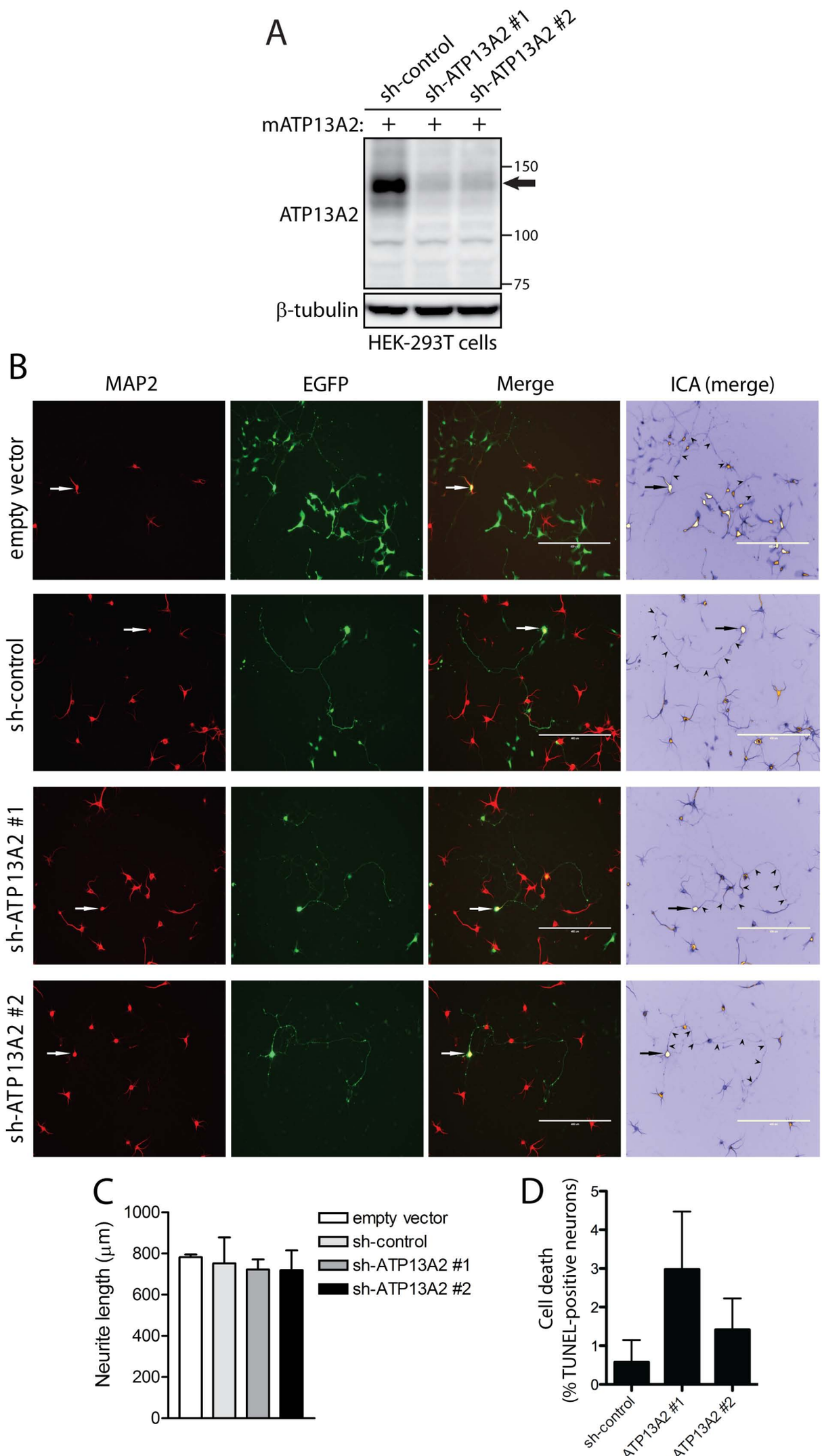
A
sh-control
sh-ATP13A2 #1
sh-ATP13A2 #2
mATP13A2: + + +
ATP13A2
150
100
75
β-tubulin
HEK-293T cells
B
MAP2
EGFP
Merge
ICA (merge)
empty vector
sh-control
sh-ATP13A2 #1
sh-ATP13A2 #2
C
Neurite length (μm)
1000
800
600
400
200
0
empty vector
sh-control
sh-ATP13A2 #1
sh-ATP13A2 #2
D
Cell death
(% TUNEL-positive neurons)
5
4
3
2
1
0
sh-control
sh-ATP13A2 #1
sh-ATP13A2 #2

Figure S3

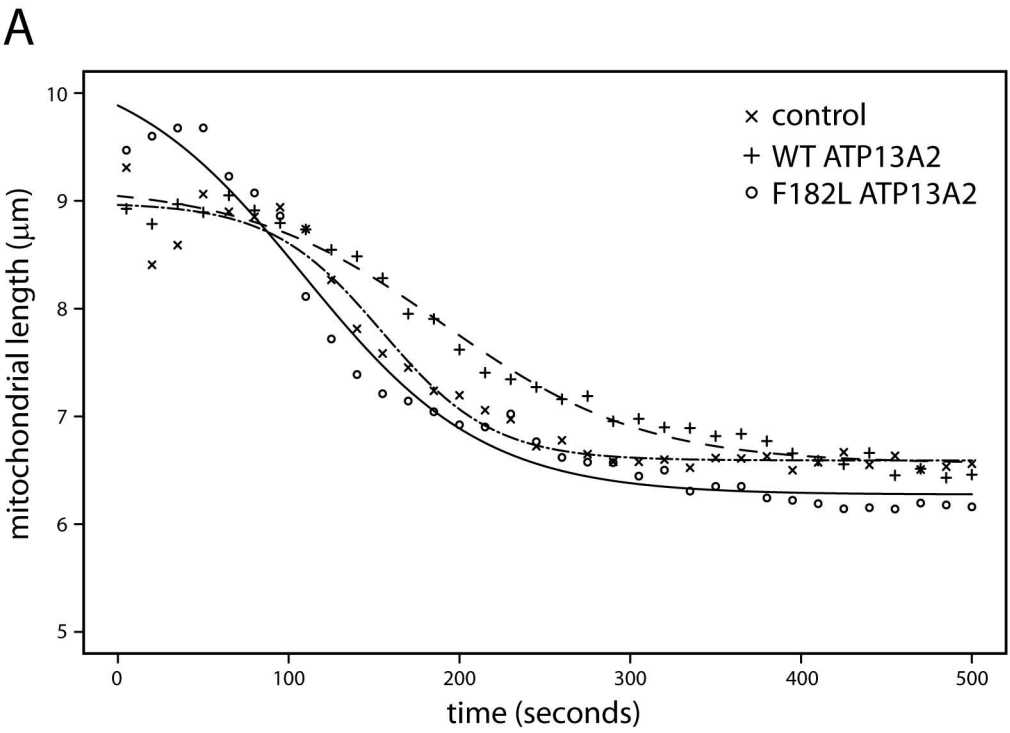
A
mitochondrial length (μm)
time (seconds)
× control
+ WT ATP13A2
o F182L ATP13A2

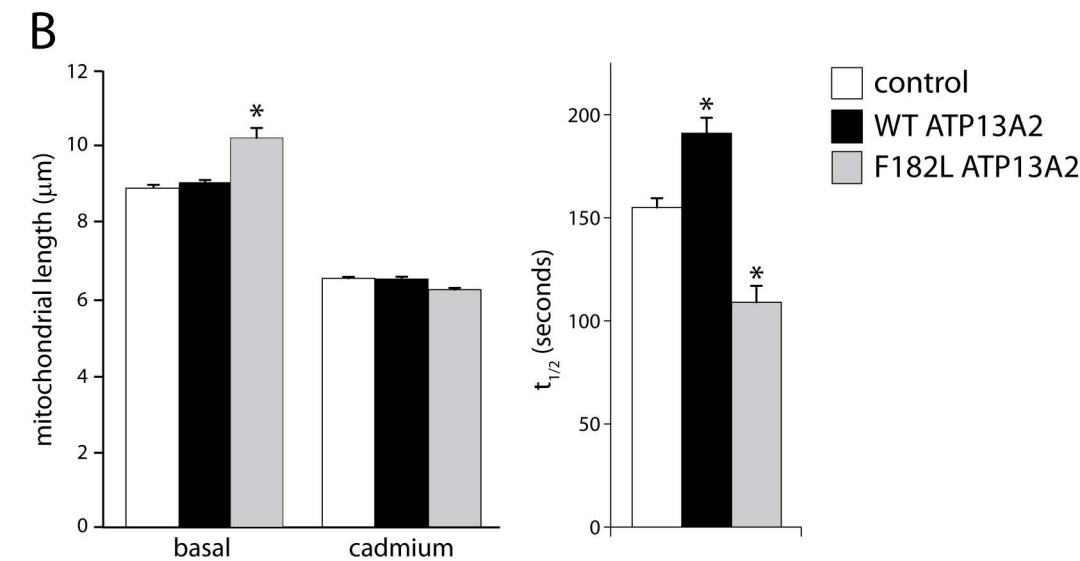
B
mitochondrial length (μm)
basal
cadmium
t1/2 (seconds)
control
WT ATP13A2
F182L ATP13A2

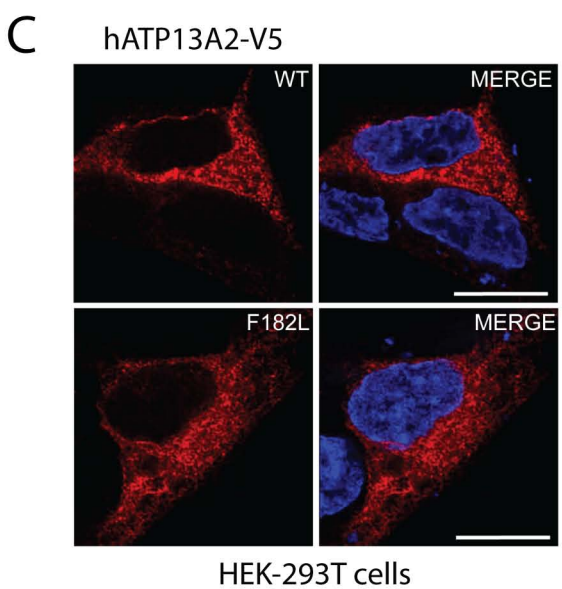
C
hATP13A2-V5
WT
MERGE
F182L
MERGE
HEK-293T cells

Figure S4

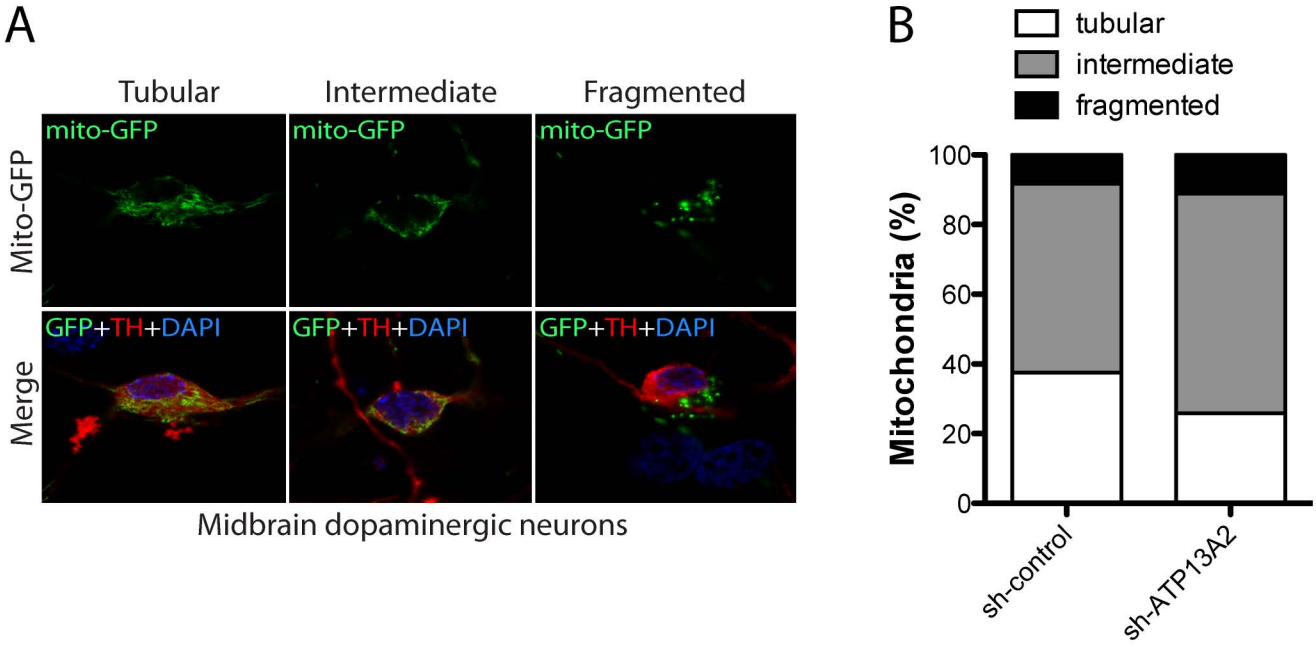
A
Tubular
Intermediate
Fragmented
Mito-GFP
Merge
mito-GFP
mito-GFP
mito-GFP
GFP+TH+DAPI
GFP+TH+DAPI
GFP+TH+DAPI
Midbrain dopaminergic neurons
B
tubular
intermediate
fragmented
Mitochondria (%)
100
80
60
40
20
0
sh-control
sh-ATP13A2

Figure S5